

Endocrinology

endo.endojournals.org

Published online before print August 4, 2010, doi: 10.1210/en.2010-0623
Endocrinology **October 1, 2010** vol. 151 no. 10 **4705-4716**

Home | 2010 Archive | October 2010 | Tsuchiya et al. 151 (10): 4705

DIABETES-INSULIN-GLUCAGON-GASTROINTESTINAL

**Cholesterol Biosynthesis Pathway
Intermediates and Inhibitors Regulate
Glucose-Stimulated Insulin Secretion and
Secretory Granule Formation in Pancreatic β
-Cells****Miho Tsuchiya¹, Masahiro Hosaka¹, Tomohisa Moriguchi, Shaojuan Zhang,
Masayuki Suda, Hiromi Yokota-Hashimoto, Kazuo Shinozuka and Toshiyuki Takeuchi** Author Affiliations

Secretion Biology Lab (M.T., M.H., S.Z., M.S., H.Y.-H., T.T.), Institute for Molecular and Cellular Regulation, Gunma University, Maebashi 371-8512, Japan; and Department of Chemistry and Chemical Biology (T.M., K.S.), Graduate School of Engineering, Gunma University, Kiryu 376-8515, Japan

Address all correspondence and requests for reprints to: Toshiyuki Takeuchi, Department of Molecular Medicine, Institute for Molecular and Cellular Regulation, Gunma University, 3-39-15 Showa-machi, Maebashi 371-8512, Japan. E-mail: tstake@showa.gunma-u.ac.jp.**Abstract**

Cholesterol is reportedly abundant in the endocrine secretory granule (SG) membrane. In this study, we examined the involvement of cholesterol biosynthesis intermediates and inhibitors in insulin secretion and SG formation mechanisms. There are two routes for the supply of cholesterol to the cells: one via *de novo* biosynthesis and the other via low-density lipoprotein receptor-mediated endocytosis. We found that insulin secretion and content are diminished by β -hydroxy- β -methylglutaryl-coenzyme A inhibitor lovastatin but not by lipoprotein depletion from the culture medium in MIN6 β -cells. Cholesterol biosynthesis intermediates mevalonate, squalene, and geranylgeranyl pyrophosphate enhanced glucose-stimulated insulin secretion, and the former two increased insulin content. The glucose-stimulated insulin secretion-enhancing effect of geranylgeranyl pyrophosphate was also confirmed in perfusion with rat islets. Morphologically, mevalonate and squalene increased the population of SGs without affecting their size. In contrast, lovastatin increased the SG size with reduction of insulin-accumulating dense cores, leading to a decrease in insulin content. Furthermore, insulin was secreted in a constitutive manner, indicating disruption of regulated insulin secretion. Because secretogranin III, a cholesterol-binding SG-residential granin-family protein, coincides with SG localization based on the cholesterol composition, secretogranin III may be associated with insulin-accumulating mechanisms. Although the SG membrane exhibits a high cholesterol composition, we could not find detergent-resistant membrane regions using a lipid raft-residential protein flotillin and a fluorescent cholesterol-Si-pyrene probe as markers on a sucrose-density gradient fractionation. We suggest that the high cholesterol composition of SG membrane with 40–50 mol% is crucial for insulin secretion and SG formation functions.

Endocrine secretory granules (SGs) store peptide hormones together with their associating proteins such as granin-family proteins and prohormone-converting enzymes (1). SGs exhibit a characteristic feature in their membrane, a strikingly high level of cholesterol composition (2, 3). In the literature, synaptic vesicle membranes are known to be composed of a high cholesterol level, 25–35 mol% (3, 4). However, the measured cholesterol composition of SG membranes was much higher than that of synaptic vesicle membranes, that is, 37–45 mol% in the three popular endocrine cell lines (3), and furthermore, it was 65 mol% in bovine pituitary neural lobe SG membranes (2). Thus, the SG membrane is thought to have the highest cholesterol levels among the cellular organelle membranes.

Cholesterol is supplied into cells via two routes: one via *de novo* biosynthesis from acetyl-coenzyme A (CoA) by the multi-enzyme pathway on the endoplasmic reticulum (ER) and the other via extracellular transport into cells by low-density lipoprotein (LDL)-mediated endocytosis (5). In the *de novo* biosynthesis route, cholesterol is synthesized from acetyl-CoA in a complex series of reactions via the limiting step reaction of β -hydroxy- β -methylglutaryl (HMG)-CoA to mevalonate by HMG-CoA reductase. Mevalonate is converted to the active isoprenoid unit, five-carbon isoprenyl pyrophosphate, which is then condensed to form the 10-carbon intermediate, geranyl pyrophosphate. A further condensation with isoprenyl pyrophosphate forms 15-carbon farnesyl pyrophosphate (FPP). The two FPPs are condensed to the 30-carbon noncyclic squalene, which is cyclized to yield the steroid ring and side chain and subsequently results in the final 27-carbon product, cholesterol. Along with this main route, FPP branches into two routes: farnesylation of small GTP-coupling (G) protein Ras and geranylgeranylation of small G proteins Rho, Rac, and

Rab (6, 7) (Supplemental Fig. 1, published on The Endocrine Society's Journals Online web site at <http://endo.endojournals.org>). In particular, this geranylgeranylated small G protein is known to regulate intracellular traffic of SGs (6, 7). For example, Rab3a and Rab27a were demonstrated to play a crucial role in formation, trafficking, and tethering of the SGs in β -cells (8, 9). Cdc42 and Rac1 were proposed as a specific mediator for insulin secretion (10, 11). The dominant-negative mutant of farnesyl transferase/geranylgeranyl transferase was shown to inhibit insulin secretion in INS 832/13 cells (12).

When cholesterol is synthesized on the ER, it is transported to the plasma membrane via the Golgi apparatus (13, 14). During the transport to the plasma membrane, cholesterol forms a gradient in composition from the ER membrane (approximately 5 mol%) to the plasma membrane (20–30 mol%) (13, 14, 15). Thus, as described above, the cholesterol composition in the SG membrane is strikingly high (2, 3). Because some SG-residential proteins, such as secretogranin III (SgIII), carboxypeptidase E (CPE), and prohormone convertases PC1/3 and PC2, have high affinity to cholesterol (2, 16, 17, 18, 19), cholesterol may play essential roles in sorting these proteins into the SGs (20, 21).

In this study, we examined the effect of cholesterol biosynthesis pathway intermediates mevalonate, squalene, and geranylgeranyl pyrophosphate (GGPP), and of HMG-CoA reductase inhibitor lovastatin on glucose-stimulated insulin secretion (GSIS) and SG formation capacity. We found that mevalonate and squalene increase both insulin secretion and SG formation capacity, whereas GGPP increases insulin secretion both from MIN6 β -cells and rat islets, but it did not affect insulin content. On the contrary, lovastatin impeded regulated insulin secretory function severely. We further examined the possibility of the detergent-resistant membrane (DRM) region on the SG membrane using a novel fluorescent probe, cholesterol-Si-pyrene (22).

Materials and Methods

MIN6 β -cell culture and islet isolation

We used a mouse pancreatic β -cell line, MIN6, cultured in DMEM with 15% fetal bovine serum (FBS) and 50 μ M 2-mercaptoethanol. We used early-passage MIN6 cells before passage 20, because they were shown to decrease the SG number with successive passages (23).

Islets were isolated from Wistar rats by pancreatic duct injection of 1.33 mg/ml collagenase solution (type XI; Sigma-Aldrich, St. Louis, MO) followed by digestion at 37 °C for 9–12 min with mild shaking. Islets were picked up by hand selection under a dissecting microscope. Rats were housed in a specific-pathogen-free facility and given free access to water and food. We conducted our animal experiments in accordance with the Guidelines for the Care and Use of Laboratory Animals of the Medical Research Council, Gunma University.

Secretion function assays by cholesterol biosynthesis pathway intermediates and inhibitors

For insulin secretion assay, MIN6 cells were cultured in a 100-mm plastic plate until 80% confluency. Because FBS contains cholesterol-carrying lipoprotein, we used lipoprotein-depleted fetal calf serum (LPDS; Biowest, Nuaille, France) (24) to examine the effect of endogenous cholesterol alone. For cholesterol biosynthesis pathway intermediates (Supplemental Fig. 1; each reaction is numbered), we used mevalonate [(–)-mevalonolactone; Sigma-Aldrich] (25), squalene (Sigma-Aldrich) (26), cholesterol-PEG600 (Sigma-Aldrich; 27), and GGPP ammonium salt (Sigma-Aldrich) (28). To suppress specific reactions on the cholesterol biosynthesis pathway, we used HMG-CoA reductase inhibitor lovastatin (Wako, Osaka, Japan) (2), geranylgeranylation reaction inhibitor GGTI-2147 (geranylgeranyl transferase inhibitor-2147) (12), and farnesylation reaction inhibitor FTI-277 (farnesyl transferase inhibitor) (29), as indicated in the figure legends. Insulin secretion assay was performed either in a low glucose (LG, 2 mM) or in high glucose (HG, 25 mM) condition in the Krebs-Ringer (KR) buffer for 30 min.

Isolation of the SG fraction by sucrose density gradient centrifugation

To collect SGs, the insulin peak was identified in the fractionated samples (16). Briefly, cell homogenate was centrifuged at 3000 \times g for 2 min. The resulting supernatant, a crude organelle fraction, was layered onto the sucrose density gradient (20–70%, wt/vol), and centrifuged at 113,000 \times g for 19 h at 4 °C in a swing rotor. Gradients were divided into 16 fractions by piston displacement.

Labeling with a fluorescent cholesterol probe and cell fractionation

MIN6 cells were cultured with 10 or 50 μ M pyrene-Si-cholesterol (22) for 2 h and then fractionated into 16 samples by 20–70% sucrose density gradient (16). The fluorescence intensity of each fraction was measured by the fluorometer FL2500 (Hitachi, Tokyo, Japan) with an excitation wavelength of 322 nm and an emission wavelength of 377 nm.

Cell death assay

Cell death of MIN6 was measured by trypan blue dye exclusion assay. The assay was performed on FBS, LPDS, mevalonate, squalene, GGPP, lovastatin, FTI-277, GGTI-2147, GGTI-298 (30), cholesterol-PEG600 (27), methyl- β -cyclodextrin (m β CD)-cholesterol complex (31), and 7-ketocholesterol, a typical oxysterol (32). We used the resulting cell death data to determine the dosage of additives for insulin secretion assay and morphological examination.

Perfusion assays

Perfusion assays were performed using isolated rat islets (33). The 2.5-ml syringe was cut to a volume of 700 μ l, and the bottom was plugged with Sephadex G-25 gel (GE Healthcare, Piscataway, NJ). To this handmade column, 50 islets were placed on the gel. This column was eluted with the LG-KR buffer [15 mM HEPES (pH 7.4), 120 mM NaCl, 5 mM KCl, 2 mM CaCl₂, 1 mM

MgCl₂, 24 mM NaHCO₃, 0.1% BSA, and 2.8 mM glucose] at a constant flow rate of 1.0 ml/min for 40 min, stabilizing insulin basal secretion from islets. During the perifusion experiment, islets were stimulated with the 16.7 mM HG-KR buffer for 15 min three times. Between the first and second HG stimulations, the islets were perfused with or without 10 μM GGPP in the RPMI 1640 medium at a constant flow rate of 1.0 ml/min for 2 h. Furthermore, between the second and third HG stimulations, the islets were perfused again with the RPMI 1640 medium for 1 h to get rid of GGPP effect. During the whole perifusion, samples were collected every 1 min for insulin assay.

Immunoelectron microscopy

MIN6 cells were first fixed with 1% glutaraldehyde-2% paraformaldehyde in 0.1 M cacodylate buffer (pH 7.4) for 1 h on ice. The scraped cells were centrifuged to pellets and dehydrated with 70% ethanol and infiltrated into pure LR White resin (London Resin, Hampshire, UK) for 12 h at 4 C. The pellets were then placed in gelatin capsules with fresh LR White resin and polymerized for 72 h at 55 C. For Immunogold, ultrathin sections from cell blocks were incubated for 12 h at 4 C with the guinea pig first antisera to insulin (Sigma-Aldrich; diluted 1:1500), followed by the goat anti-guinea pig IgG (BBIInternational, Cardiff, UK) conjugated with colloidal gold particles (10 nm in diameter). The sections were contrasted with saturated aqueous solutions of uranyl acetate and lead citrate and examined with a JEM-1010 electron microscope (JEOL Ltd., Tokyo, Japan). The granular diameter was measured, and 19 representative sections (one section is ~100 μm²) were counted. The diameter of each elliptic granule was calculated as an average of the longer elliptic diameter and the smaller elliptic diameter.

Cholesterol and phospholipids assays

Cholesterol composition in the SG membrane was measured as described previously (3). Briefly, we used the Bligh-Dyer method to extract the lipids from the SG membranes. For the phospholipid quantitative assay, the phospholipid of an extracted lipid was analyzed by its absorbance at 820 nm. For the cholesterol quantitative assay, a thin-layer chromatography plate (Silica gel 60; Merck, White Station, NJ) was used to separate cholesterol in an extracted lipid. Mol% is used to express a cholesterol composition ratio when a mol number of total lipids is assumed to be 100.

Labeling with [³H]GGPP

[1-(n)-³H] GGPP triammonium salt (15.0 Ci/mmol) was purchased from Amersham-Pharmacia Biotech (Piscataway, NJ). MIN6 cells in six-well dishes were labeled by 12.5 μCi of [³H]GGPP with or without 10 μM lovastatin for 16 h. After labeling, cells were extracted by the buffer (IEF solution; Invitrogen, Carlsbad, CA) containing 7.7 M urea, 2.2 M thiourea, and 4.4% CHAPS. The procedure for two-dimensional (2-D) gel electrophoresis and immune blotting was performed according to the manufacturer's specification (Invitrogen). Briefly, cell extract was subjected to a ZOOM Strip pH3-10L using the ZOOM IPGRRunner (Invitrogen) as the first dimension. Then, for the second dimension, SDS-PAGE was performed on NuPAGE Novex 4–12% Bis-Tris ZOOM gel (Invitrogen). The ³H signals of SDS-PAGE were recorded using BAS-1800II (Fujifilm, Tokyo, Japan).

Isolation of detergent-resistant membrane (DRM) fraction

DRM fractions were prepared by DRM sucrose gradient centrifugation (34). As a detergent, 1% Triton X-100 was used. After MIN6 cells were cultured for 2 h with 50 μM pyrene-Si-cholesterol, they were extracted with 1% Triton X-100/MN buffer [25 mM 2-(N-morpholino)ethanesulfonic acid NaOH (pH 6.5), 0.15 M NaCl, and protease inhibitors] on ice for 30 min. The extracts were adjusted to 42.5% sucrose in a volume of 1 ml. The extract was underlaid with 7 ml of 10–30% sucrose gradient and centrifuged at 75,000 × g for 20 h. After centrifugation, fractions (0.5 ml each) were collected from the bottom of a centrifuge tube. An equal volume of each fraction was run on an SDS-PAGE for immunoblotting with anti-flotillin-1 (1:2000) and CPE (1:2000) antibodies.

Statistical analysis

Mean ± SE bars are added to each graph. Statistical analysis is performed by ANOVA and *post hoc* comparisons for Figs. 1C, 2A, 2B, 2D, 3A, 4A, 6A, and 6E and Supplemental Figs. 2 and 5D and Student's *t* tests for Figs. 1B and 2C. A value of *P* < 0.05 was considered significant. Statistical significance is indicated in each figure legend.

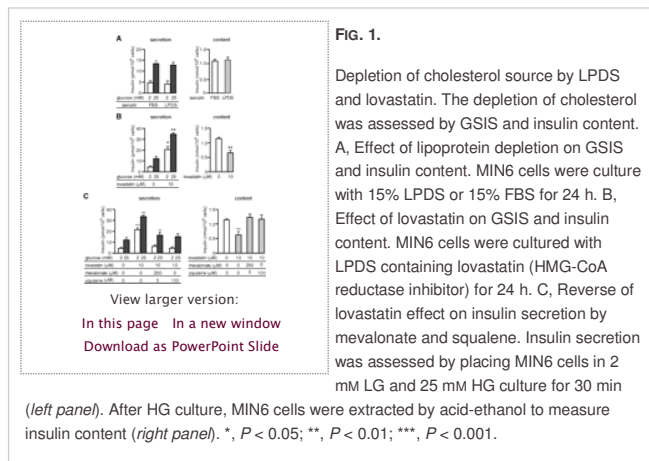
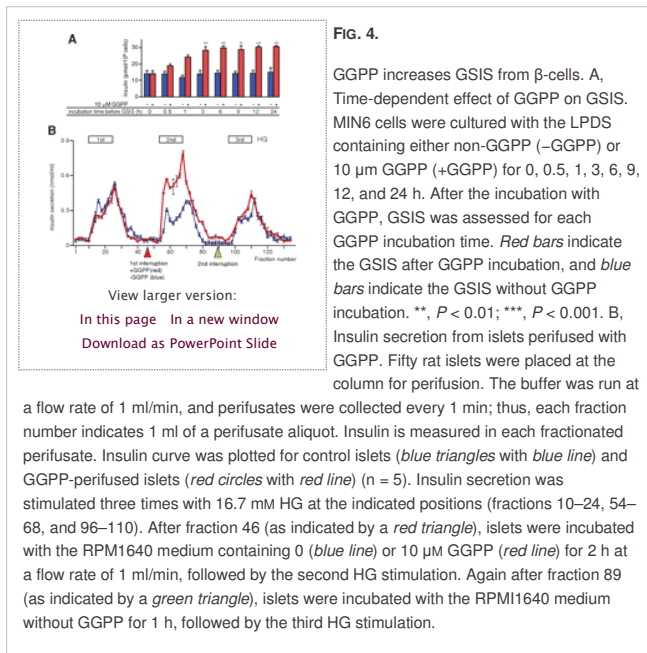
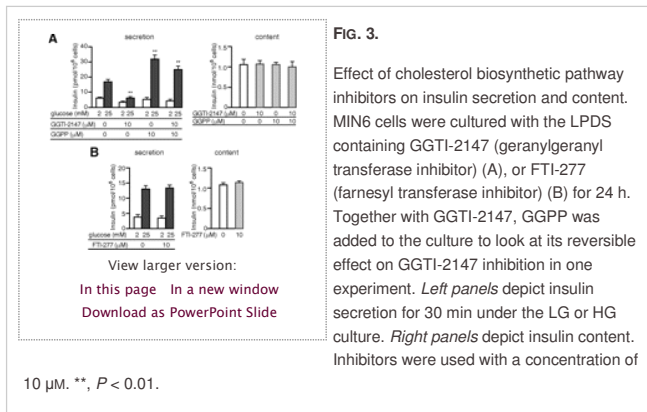
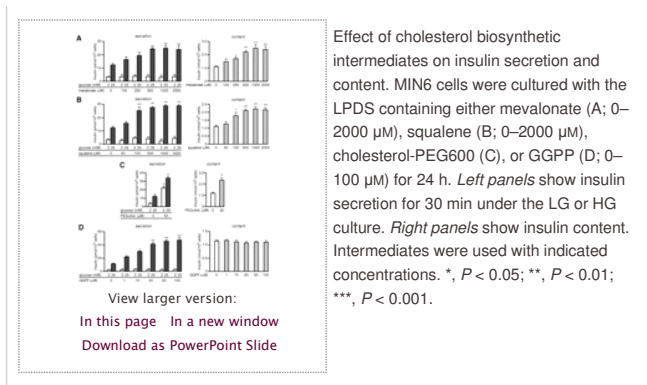


FIG. 2.



Results

Participation of exogenous and endogenous cholesterol to SG membranes

Recent studies suggest that cholesterol affects insulin secretion and SG formation (2, 3, 35). Cholesterol is supplied to the cell by two routes: one by LDL-receptor-mediated uptake and the other by *de novo* synthesis for which HMG-CoA reductase is a key step (Supplemental Fig. 1). We initially depleted exogenous cholesterol using LPDS instead of FBS (Fig. 1A). Insulin secretion resulted in no difference between 2 mM LG and 25 mM HG culture for 30 min, and net insulin content was also unchanged by the LPDS culture. We then looked at the effect of cholesterol depletion on insulin secretion and content by inhibiting HMG-CoA reductase with lovastatin (Fig. 1B). Both basal and HG-stimulated insulin secretions were elevated by 10 μM lovastatin. However, substantial increase in basal constitutive secretion suggests disruption of the regulated insulin secretion, as was exemplified by the expression experiment with the cholesterol-binding domain-deleted SgIII (36). Thus, net increase in HG-stimulated insulin secretion appeared to result from insulin release through fragile lipid bilayer membranes of SGs and plasma membranes by the statin. Insulin content was significantly decreased to almost half of that of the control level perhaps due to the leak through fragile membranes. Statin-induced abnormal increase in apparent insulin secretion and decrease in insulin content were rescued by the addition of cholesterol biosynthesis

intermediates mevalonate or squalene (Fig. 1C†). Therefore, the decrease in *de novo* synthesized cholesterol and/or its intermediate levels appears to result in the dysfunction of regulated insulin secretion from MIN6 β -cells.

Insulin secretion and content by cholesterol biosynthetic intermediates

To supply hydrophobic lipid cholesterol to the cells, it is necessary to use a water-soluble cholesterol-PEG600 (27) or a cholesterol carrier polymer m β CD (31) for cholesterol delivery to the cells. However, m β CD-cholesterol complex is toxic to the MIN6 cells (Supplemental Fig. 2). Thus, we selected cholesterol-PEG600 and nontoxic cholesterol biosynthesis intermediates mevalonate, squalene, and GGPP for evaluating insulin secretion and content. MIN6 cells were cultured in the LPDS medium containing either mevalonate or squalene. With mevalonate, GSIS was significantly increased to two times over that of the no-mevalonate control value up to 500 μ M. Basal insulin secretion was not affected by mevalonate. Unexpectedly, insulin content with mevalonate was significantly increased to over two times more than that of the control value (Fig. 2A†). Because mevalonate is an intermediate in the first part of the cholesterol biosynthetic pathway, it is hard to identify its effective points on the biosynthesis route including branching routes after mevalonate. Thus, we selected squalene for its effect on insulin secretion. Although squalene is hydrophobic like cholesterol, it is soluble to dimethylsulfoxide, unlike cholesterol. Similar to mevalonate, squalene extensively affected regulated insulin secretion (Fig. 2B†). GSIS increased to 2.4 times over that of the no-squalene control value by 1000 μ M squalene (Fig. 2B†, left panel). Insulin content also increased two times over that of the control value by 1000 μ M squalene (Fig. 2B†, right panel). However, basal insulin secretion was unchanged. Cholesterol-PEG600 increased both basal and HG-stimulated insulin secretion (Fig. 2C†), similar to lovastatin (Fig. 1B†). It also increased insulin content almost two times over that of the control value in contrast to lovastatin (Fig. 2C†). However, cholesterol-PEG600 was cytotoxic to MIN6 cells (Supplemental Fig. 2), which was similar to lovastatin. Thus, a marked increase or decrease of cholesterol composition in the membrane appears to induce a cytotoxic effect.

Mevalonate is a five-carbon isoprenyl pyrophosphate, which is condensed to 15-carbon FPP. FPP is a key intermediate product not only for cholesterol but also for protein prenylation (farnesylation and geranylgeranylation) (Supplemental Fig. 1). From FPP, the major pathway produces the 30-carbon noncyclic squalene by the condensation of two FPPs. Another pathway is involved in production of prenylated small GTP-binding proteins. To examine the effects of protein geranylgeranylation on insulin secretion and content, MIN6 cells were cultured in the LPDS medium with up to 100 μ M GGPP (Fig. 2D†). HG-induced insulin secretion increased up to 4.5 times over that of the control level in a dose-dependent manner, whereas basal insulin secretion was unaffected by any dosage of GGPP (Fig. 2D†, left). Insulin content was unaffected by GGPP, unlike it was by mevalonate and squalene (2D, right).

Insulin secretion and content by cholesterol biosynthesis pathway inhibitors

We next examined the involvement of FPP-originated side pathway inhibitors in insulin secretion and content. Because we have already looked at the enhancing effect of GGPP on regulated insulin secretion (Fig. 2D†), we next examined the effect of geranylgeranyl transferase inhibitors GGTI-2147 and GGTI-298 and farnesyl transferase inhibitor FTI-277 on insulin SG functions. Although GGTI-2147 did not affect MIN6 cell survival, GGTI-298 was toxic to the cells (Supplemental Fig. 2). Thus, we used GGTI-2147, which decreased HG-induced insulin secretion, whereas it did not affect basal insulin secretion. The GGTI-2417-mediated inhibitory effect on GSIS was reversed by 10 μ M GGPP (Fig. 3A†, left). However, insulin content remained unchanged with or without GGTI-2147 or GGPP (Fig. 3A†, right). In contrast, FTI-277 was ineffective in altering insulin secretion and content (Fig. 3B†). Thus, the branching route to Ras family protein farnesylation appears not to be involved in insulin secretion.

GGPP enhances GSIS from β -cells

Because GGPP enhances GSIS without increasing insulin content, we presumed that GGPP is effective as an insulinotropic chemical. Initially, we looked at HG-stimulated insulin secretion from the MIN6 cells after incubation with GGPP for up to 24 h. GGPP-incubated MIN6 cells secreted higher levels of insulin by HG stimulation, which reached almost two times more over that of the no-GGPP value (Fig. 4A†). Thus, GGPP is effective in increasing GSIS.

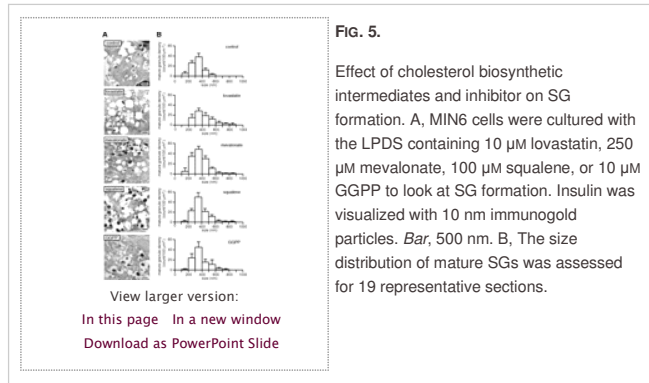
We next confirmed this potency with rat islets. Rat islets were perfused with 2.8 mM LG-KR buffer for 10 min to obtain stable basal insulin secretion. Islets were then perfused with the 16.7 mM HG-KR buffer for 15 min. We repeated this LG and HG cycle three times. To examine the effect of GGPP, we incubated islets with 10 μ M GGPP in LG-KR buffer for 2 h before the second HG cycle (Fig. 4B†). As a control, islets were also perfused by the LG-KR buffer without GGPP. In the non-GGPP condition, insulin peak decreased with the advancement of HG-stimulation cycle; that is, the first response is followed by the lower second response, which was followed by the even lower third response (Fig. 4B†, blue line). In contrast, when GGPP was incubated before the second cycle, insulin peak was elevated higher than the first cycle peak by the non-GGPP buffer (Fig. 4B†, red line). The GGPP-induced insulin peak reached approximately 2-fold higher than the second cycle peak without GGPP, suggesting that GGPP is potent for inducing insulin secretion. Separately, when we incubated 10 μ M GGPP for 2 h before the perfusion, the first and second insulin peaks by HG became 1.5- to 2.0-fold higher than the non-GGPP control peak (Supplemental Fig. 3). After the perfusion experiments, islets were extracted for insulin. Insulin content was 194 pmol/50 islets with GGPP (SD = 0.42) and 186 pmol/50 islets without GGPP (SD = 0.07). Thus, it was demonstrated that GGPP did not increase insulin content in rat islets.

Because GGPP increased insulin secretion from rat islets, we next screened GGPP-targeted proteins in MIN6 cells by 2-D gel mapping. MIN6 cells were metabolically labeled by [3 H]GGPP. Cell extracts were subjected to both SDS-PAGE and 2-D gel electrophoresis for fluorography. A fluorography image showed that most 3 H-labeled proteins were at 25–30 kDa (Supplemental Fig. 4A). Over 15 [3 H]geranylgeranylated proteins were identified on the 2-D autoradiogram between a

size of 10 and 30 kDa (Supplemental Fig. 4B). Rab27a/b appeared to correspond well to a radioactive spot. But, immunoprecipitation of Rab27a/b from the cell extract did not erase the Rab27a/b band (Supplemental Fig. 4C), suggesting that Rab27a/b is not a geranylgeranylation target. Other well-known geranylgeranylated proteins, Rab3a, Cdc42, and Rac1, were identified on the 2-D gel by immunoblotting, and their immunoblot spots were separated from the marked radioisotope spots (Supplemental Fig. 4B). Furthermore, the Rab3a band did not disappear after the immunoprecipitation by anti-Rab3a from the extract (Supplemental Fig. 4C). Although we could not identify unknown types of small G proteins, they were thought to be involved in increasing GSIS.

Effect of cholesterol biosynthetic pathway intermediates on SG formation

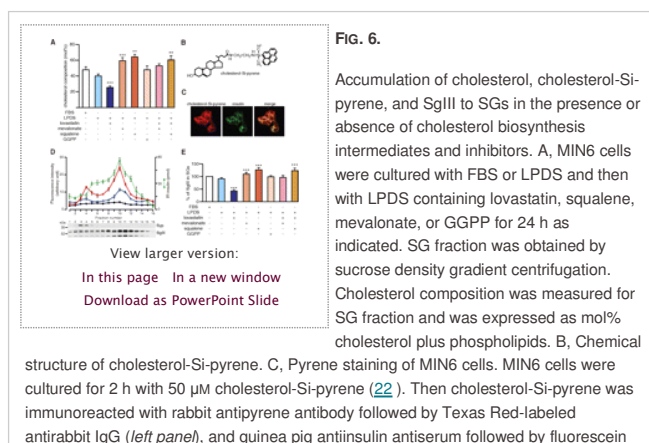
We next examined the effect of cholesterol biosynthetic intermediates on SG formation and morphological feature by immunoelectron microscopy. We defined a mature SG by the presence of a dense core with at least five colloidal gold particles indicative of insulin. Marked morphological changes were not observed, but dense cores appeared to be increased by mevalonate, squalene, and GGPP. On the other hand, lovastatin resulted in a longer SG diameter in comparison with that of the nonadditive control, and dense cores shrunk and disappeared (Fig. 5A).



We then evaluated a relative population of mature SGs on 19 sections ($\sim 100 \mu\text{m}^2 \times 19$ sections) (Fig. 5B). Mevalonate increased the population of SGs with a diameter of 200–500 nm. Likewise, squalene increased the SG population with 300–400 nm. On the other hand, lovastatin decreased the population of this range, but it increased the population over 500 nm. However, GGPP did not affect the distribution of SG size. The total population of SGs was 84.2 ± 10.7 and 61.4 ± 16.4 per $100 \mu\text{m}^2$ for the control and lovastatin groups, respectively ($P < 0.05$). In contrast, mevalonate and squalene increased the SG population to 128.9 ± 19.0 and 117.7 ± 15.8 per $100 \mu\text{m}^2$, respectively ($P < 0.01$). However, GGPP was similar to that of the control in terms of SG distribution (95.0 ± 15.8 vs. 84.2 ± 10.7 per $100 \mu\text{m}^2$, $P > 0.05$).

Cholesterol composition, its supply routes, and SgIII accumulation to SGs

Because we observed morphological and numerical changes in SGs by cholesterol synthetic pathway intermediates and inhibitors, we therefore examined the cholesterol composition of SGs. SGs were collected from the insulin peak fraction by sucrose density gradient centrifugation. Cholesterol composition was not significantly altered between FBS and LPDS culture, although it was a little lower in the LPDS culture than that in the FBS culture, suggesting less involvement of exogenous cholesterol as a constituent of SG membranes (Fig. 6A). Cholesterol composition was 48, 40, 24, 59, 64, 48, 51, and 59 mol% in FBS, LPDS, lovastatin, mevalonate, squalene, GGPP, lovastatin plus mevalonate, and lovastatin plus squalene, respectively (Fig. 6A). Mevalonate and squalene increased the cholesterol composition of the SGs; thus, they must have been used for the synthesis of cholesterol. In contrast, lovastatin decreased the SG cholesterol composition significantly, suggesting the blocking of the *de novo* cholesterol synthesis results in the cholesterol depletion in the SG membranes. This lovastatin-induced decrease in cholesterol composition was recovered by mevalonate and squalene, suggesting that post-HMG-CoA reductase intermediates are able to rescue the blockade of the cholesterol biosynthesis route by lovastatin. GGPP did not affect SG cholesterol composition, perhaps due to its location on the branching pathway (Supplemental Fig. 1).



isothiocyanate-labeled anti-goat IgG (*middle panel*). Merged images of cholesterol-Si-pyrene (*red*) and insulin (*green*) staining are indicated on the *right panels*. Note that cholesterol-Si-pyrene is partially colocalized with punctately stained insulin granules, which appear yellow on the *right panel*. D, Crude extract of MIN6 cells loaded with none (*black squares*), 10 μM (*blue triangles*), or 50 μM (*red circles*) of cholesterol-Si-pyrene which was fractionated via linear sucrose density gradient centrifugation. Sixteen fractions were obtained, and the fluorescence intensity of cholesterol-Si-pyrene was measured for each fraction. The fluorescent peak appeared at fractions 4 and 9–11. The latter higher peak was overlapped with the insulin peak. Fractionated samples were marked with the immunoblot of the SLMV-residential protein, synaptophysin and SG-residential protein, SgIII. E, A part of the SG fraction was run on an SDS-PAGE for immunoblotting with anti-SgIII and β -actin antibodies to obtain SgIII content (*upper panel*). SgIII and β -actin were quantified by NIH Image (*lower panel*). All experiments were independently repeated at least three times. **, $P < 0.01$; ***, $P < 0.001$. IR, Immunoreactive.

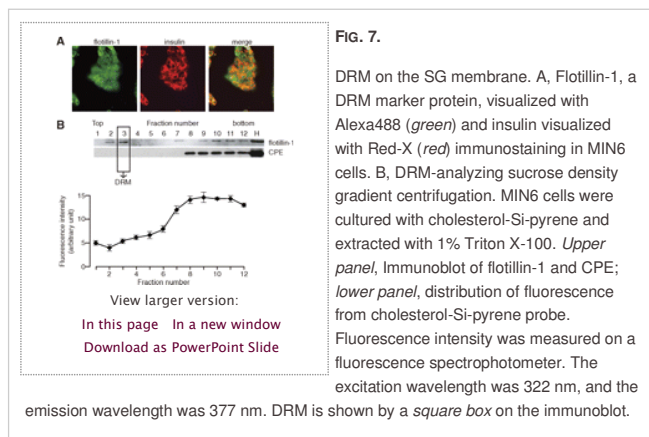
To further investigate the involvement of exogenous cholesterol in an SG membrane constituent, we used a novel fluorescent cholesterol analog, cholesterol-Si-pyrene (22) (Fig. 6B) for the MIN6 culture. Cholesterol-Si-pyrene accumulates at the SGs, and it has been shown to overlap with insulin-positive granules (Fig. 6C). We separated the subcellular organelles of MIN6 cells to observe the cholesterol-Si-pyrene distribution by sucrose density gradient centrifugation. Cholesterol-Si-pyrene accumulated at the SG fraction indicated by the insulin peak in a probe dosage-dependent manner (Fig. 6D). Thus, exogenous cholesterol is supplied to the SG membrane, although the incorporation ratio of exogenous cholesterol might be small compared with the endogenous one. Cholesterol-Si-pyrene was also incorporated to the synaptic-like microvesicle (SLMV) fraction. Interestingly, synaptic vesicle-residential protein synaptophysin was reported to bind to cholesterol (37) and was also localized to the SLMV fraction in β -cells (3).

Because SgIII binds to cholesterol in the SG membrane (16), we next examined SgIII content at SGs in the presence of mevalonate, squalene, GGPP, or lovastatin (Fig. 6E). Squalene increased SgIII content at SGs, whereas other intermediates did not increase it. Remarkably, lovastatin decreased SgIII content, suggesting that the cholesterol depletion prevents SgIII accumulation to SGs because of its cholesterol-binding capacity. This lovastatin-induced decrease in SgIII accumulation was recovered by mevalonate and squalene, as expected. In general, SgIII accumulation to SGs appears to reflect the cholesterol composition of SG membranes.

Interestingly, mevalonate and squalene did not affect the insulin biosynthesis at both transcriptional and translational levels (Supplemental Fig. 5), but they increase SG membrane cholesterol composition, leading to the accumulation of SgIII molecules with insulin peptides in SGs (20, 36).

Characteristics of the cholesterol-rich SG membrane

Because SG membranes are composed of a high level of cholesterol (Fig. 6A), we examined detergent solubility of SG membranes with a cholesterol-Si-pyrene probe. We used an antibody against flotillin-1, a protein that is enriched in DRM, as its marker (34). Flotillin-1 was widely spread over the cytoplasm, whereas insulin was stained in a punctate manner, suggesting their different subcellular localization (Fig. 7A). We then analyzed MIN6 cell lysates by sucrose density gradient centrifugation to look at SG-residential components at the DRM region. The DRM fraction was identified by flotillin-1 immunoblot (Fig. 7B, upper panel). However, cholesterol-Si-pyrene was not detected at the flotillin-1-positive DRM region; instead, it was distributed over the much heavier non-DRM region by its fluorescence (Fig. 7B, lower panel). Although CPE was reported to localize in lipid rafts (2), CPE was also distributed over the non-DRM region (Fig. 7B, lower panel). Thus, SG membranes of MIN6 cells do not contain a flotillin-marked DRM region.



Discussion

Endocrine SGs consist of a high level of cholesterol in their membrane (2, 3). The cholesterol composition of SG membranes was 48 and 40 mol% in the control FBS and LPDS cultures, respectively, whereas it increased to 59 and 64 mol% with mevalonate and squalene, respectively, and it decreased to 24 mol% with lovastatin (Fig. 6A). In proportion to this change, insulin content was shifted over 50% higher with mevalonate and squalene, and it was over 40% lower with lovastatin (Figs. 1 and 2). These high membrane cholesterol composition levels seem to be maximal just before leading to cholesterol precipitation (38). In terms of SG membrane cholesterol

supply, endogenous cholesterol appeared to be a major route, because HMG-CoA reductase inhibitor lovastatin substantially reduced its composition (Fig. 6A†), although a small level of exogenous cholesterol is definitely supplied as a constituent (Fig. 6D†). Although lovastatin deteriorates SG formation, its underlying mechanism remains to be known. Recently, lovastatin was shown to activate AMP-activated protein kinase (AMPK) in endothelial cells (39). AMPK plays a key role in whole-body energy homeostasis including insulin secretion function (40, 41). However, the lovastatin effect on AMPK activation was reportedly rapid after the treatment, whereas lovastatin worked gradual and required an hour-order time course before SG cholesterol composition was lowered. Actually, lovastatin did not increase AMPK phosphorylation at the 24-h point after the lovastatin incubation in MIN6 cells (Supplemental Fig. 6). Thus, it is unlikely that statins affect SG cholesterol dynamics via AMPK activation.

Both mevalonate and squalene enhanced GSIS, insulin content, and SG membrane cholesterol composition without causing cell death (Figs. 2† and 6A† and Supplemental Fig. 2). On the cholesterol synthesis pathway, mevalonate is formed early at the six-carbon step by HMG-CoA reductase, whereas 30-carbon squalene is formed after the branching point of 15-carbon isoprenoid FPP to the prenylation pathway (Supplemental Fig. 1). For maintaining the prenylation pathway, it has been reported that a low level (less than 250 μM) of mevalonate is sufficient, and any amount over this dosage of mevalonate is processed to the major cholesterol synthesis pathway (42). Isoprenoids are used to form nonsterol products, such as dolichol, ubiquinone, and GGPP (43). These nonsterol intermediates may also contribute to SG-forming and insulin secretory functions. Thus, mevalonate serves as a substrate for cholesterol as well as for nonsterol, isoprenoid products. In contrast, squalene is destined only to the cholesterol synthesis via lanosterol (43). In humans, squalene is supplied by LDL and very-low-density lipoprotein together with cholesterol, and it is reportedly unconcerned with hypercholesterolemia because it is diffusible across the cell membrane and does not accumulate in the intracellular lipid pool (43). Thus, a very small fraction of squalene is suggested to be converted to cholesterol *in vivo*. In the culture cells, squalene concentration may be similar between the culture medium and the intracellular lipid pool, and a part of squalene may be constantly converted to cholesterol, perhaps resulting in its accumulation to the SG membrane (Fig. 2B†). However, because the flow of squalene to the cholesterol route is only partial, squalene may not cause MIN6 cell death unlike cholesterol-PEG600 (Supplemental Fig. 2). Recently, squalene epoxidase inhibitor NB-598 has attracted considerable attention as a hypercholesterolemia-curing drug (43). Because this inhibitor does not block the nonsterol isoprenoid pathway, isoprenoid-related side effects observed in statin treatments can be avoided. Xia *et al.* (44) reported that in mouse β -cells, NB-598 is reported to decrease insulin secretion and voltage-gated calcium channel function, but it did not affect SG morphology in mouse islets. It was shown that NB-598 is effective in depleting soluble *N*-ethylmaleimide-sensitive factor activating protein receptor-based lipid rafts on the plasma membrane, resulting in the impairment of insulin secretion. Thus, disruption of cholesterol-based lipid membrane structures may be different between NB-598 and statins.

Among the cholesterol synthesis sideway intermediates, GGPP is quite interesting. It is known as a substrate for small G protein geranylgeranylation for Rho, Rac, and Rab at their C-terminal cysteine residues. GGPP rescues rat primary cultured cortical neurons from cell death by lovastatin (45). In β -cells, GGPP enhances GSIS, but it does not increase insulin content (Figs. 2D†, 3A†, and 4†). To search for GGPP targets, we noted over 15 spots labeled with [^3H]GGPP in a size range of 20–30 kDa on the 2-D gel. This size range includes Rab3a, Rab27a, Cdc42, and Rac1, which are reportedly a specific mediator for insulin secretion (8, 9, 10, 11). Among these, Rab27a was identified on the 2-D gel in this study. However, Rab27a was not identified as a target, because Rab27a-immunoprecipitated MIN6 lysate also yielded this spot, as the control lysate presented it. Thus, although GGPP turned out to be insulinotropic in β -cells, its target proteins remain to be identified.

High cholesterol composition is observed in lipid rafts of the membrane, which are highly concentrated with cholesterol and glycosphingolipids. Because soluble *N*-ethylmaleimide-sensitive factor activating protein receptor proteins are reportedly associated with lipid rafts, they are implicated in the regulation of exocytosis and membrane traffic pathways (46). Tooze *et al.* (47) proposed that lipid rafts are involved in sorting SG-residential proteins to the SGs budding from the trans-Golgi network (TGN), and lipid-protein interaction is an essential process for the formation and maturation of immature SGs. Another study demonstrated that syntaxin1A and SNAP-25 are present at lipid rafts, and they regulate exocytosis of dopamine in PC12 cells (48). On the other hand, Ohara-Imaizumi *et al.* (49) investigated the relationship between syntaxin1 clusters and lipid rafts in MIN6 cells, and they showed that syntaxin1 clusters are distinct from flotillin-1-enriched DRM (31), designated by the insolubility of 1% Triton X-100. Indeed, SG-residential proteins, CPE, PC3, and PC2, have been demonstrated to exist at lipid rafts on SG membrane in AtT-20 cells (for CPE and PC3) and Neuro2a cells (for PC2) (2, 17, 18, 19). However, CPE did not show up at the DRM position; instead, it was spread along the much heavier region by DRM-analyzing sucrose density gradient centrifugation. Likewise, the cholesterol-Si-pyrene probe did not result in a peak at the flotillin-marking DRM position (Fig. 7B†). Thus, we suggest that lipid raft-like structures are unlikely to exist on the SG membranes of MIN6 β -cells.

Although the SG membrane may not have lipid raft-like structures for cholesterol, we postulate that the high cholesterol composition is essential for two functions in the SG formation. First, high cholesterol is essential for the function of SgIII (16, 36). We demonstrated that SgIII has three functional domains: the N-terminal region binds to cholesterol-rich lipid membranes (16, 36), the middle region binds to chromogranin A, which is proposed to be a hormone carrier to the SGs (1, 20, 50), and the C-terminal region binds to CPE, which is proposed to be a hormone-sorting receptor to the SGs (51). With these functions, SgIII is postulated to play an essential role in accumulating hormones and other SG-residential proteins to the high cholesterol region of the SG membranes for forming a SgIII-based chromogranin A and peptide hormone complex in the SGs budding from the TGN (20, 52). Second, cholesterol appears to regulate the SG size. Depletion of cholesterol by lovastatin increased the size of the SG (Fig. 5†). Although Wang *et al.* (35) demonstrated the appearance of an enlarged cisterna with condensed materials along the TGN in

AtT-20 cells by lovastatin treatment, we noted only enlarged SGs over 500 nm in diameter. Because the lovastatin dosage used for both experiments was 10 μ M, the difference may have been derived from the cell line used for each experiment. Furthermore, SgIII expression is well correlated with an SG cholesterol composition produced by mevalonate, squalene, and lovastatin (Fig. 6E). Notably, SgIII was decreased from the SG fraction with lovastatin. Because Farsad and De Camilli (53) suggested a possibility of cholesterol function as an initiator of lipid-driven membrane deformation, SgIII should be evaluated for its budding capacity on the TGN membrane in cooperation with cholesterol molecules. Although the high cholesterol composition of the SG membrane can be easily viewed as important in cultured β -cell lines, it is hard to evaluate this importance in animal models because the serum cholesterol level is well controlled in a narrow range by fine regulatory mechanisms with a cholesterol delivery system by lipoproteins and with a sterol regulatory element binding protein transcription system (54). Furthermore, when a cholesterol supply route is amplified by mevalonate or squalene, cellular lipid metabolism may be affected via cholesterol-responsive transcription regulators such as liver X receptor and sterol regulatory element binding protein. Because cholesterol-Si-pyrene behaves similarly to nonmodified cholesterol, endocrine cellular lipid metabolism will be further elucidated together with commercially available fluorescent phospholipids probes.

Acknowledgments

We thank Drs. H. Gomi and S. Yamada (Gunma University) for their helpful discussions and Ms. M. Hosoi and Ms. M. Kosaki for their valuable technical support.

Footnotes

This work was supported by Grants-in-Aid and the Global COE Program from the Japanese Ministry of Education, Culture, Sports, Science, and Technology.

Disclosure Summary: The authors have nothing to disclose.

First Published Online August 4, 2010

1 M.T. and M.H. contributed equally to this work.

Abbreviations: AMPK, AMP-activated protein kinase; CoA, coenzyme A; CPE, carboxypeptidase E; 2-D, two-dimensional; DRM, detergent-resistant membrane; ER, endoplasmic reticulum; FBS, fetal bovine serum; FPP, farnesyl pyrophosphate; FT, farnesyl transferase; GGPP, geranylgeranyl pyrophosphate; GGT, geranylgeranyl transferase; GSIS, glucose-stimulated insulin secretion; HMG, β -hydroxy- β -methylglutaryl; HG, high glucose; LDL, low-density lipoprotein; LG, low glucose; LPDS, lipoprotein-deficient serum; KR, Krebs-Ringer; m β CD, methyl- β -cyclodextrin; PC, prohormone convertase; SG, secretory granule; SgIII, secretogranin III; SLMV, synaptic-like microvesicle; TGN, trans-Golgi network.

Received June 3, 2010.
Accepted June 25, 2010.

References

1. **Dannies PS** 1999 Protein hormone storage in secretory granules: mechanisms for concentration and sorting. *Endocr Rev* **20**:3–21 [Abstract/FREE Full Text](#)
2. **Dhanvantari S, Loh YP** 2000 Lipid raft association of carboxypeptidase E is necessary for its function as a regulated secretory pathway sorting receptor. *J Biol Chem* **275**:29887–22993 [Abstract/FREE Full Text](#)
3. **Wang R, Hosaka M, Han L, Yokota-Hashimoto H, Suda M, Mitsushima D, Torii S, Takeuchi T** 2006 Molecular probes for sensing the cholesterol composition of subcellular organelle membranes. *Biochim Biophys Acta* **1761**:1169–1181 [Medline](#)
4. **Pfrieger FW** 2003 Role of cholesterol in synapse formation and function. *Biochim Biophys Acta* **1610**:271–280 [Medline](#)
5. **Nelson DL, Cox MM** 2005 Lipid biosynthesis. In: *Lehninger's principles of biochemistry*. 4th ed. New York: W. H. Freeman; 787–832
6. **Kowluru A** 2003 Regulatory roles for small G proteins in the pancreatic β -cell: lessons from models of impaired insulin secretion. *Am J Physiol Endocrinol Metab* **285**:E669–E684
7. **Takai Y, Sasaki T, Matozaki T** 2001 Small GTP-binding proteins. *Physiol Rev* **81**:153–208 [Abstract/FREE Full Text](#)
8. **Yaekura K, Julian R, Wicksteed BL, Hays LB, Alarcon C, Sommers S, Poitout V, Baskin DG, Wang Y, Philipson LH, Rhodes CJ** 2003 Insulin secretory deficiency and glucose intolerance in Rab3A null mice. *J Biol Chem* **278**:9715–9721 [Abstract/FREE Full Text](#)
9. **Kasai K, Fujita T, Gomi H, Izumi T** 2008 Docking is not a prerequisite but a temporal constraint for fusion of secretory granules. *Traffic* **9**:1191–1203 [CrossRef](#) [Medline](#)
10. **Nevin AK, Thurmond DC** 2005 A direct interaction between Cdc42 and vesicle-associated membrane protein 2 regulates SNARE-dependent insulin exocytosis. *J Biol Chem* **280**:1944–1952 [Abstract/FREE Full Text](#)
11. **McDonald P, Veluthakal R, Kaur H, Kowluru A** 2007 Biologically active lipids promote trafficking and membrane association of Rac1 in insulin-secreting INS 832/13 cells. *Am J Physiol Cell Physiol* **292**:C1216–1220
12. **Veluthakal R, Kaur H, Goalstone M, Kowluru A** 2007 Dominant-negative alpha-subunit of farnesyl- and geranyltransferase inhibits glucose-stimulated, but not KCl-stimulated, insulin secretion in INS 832/13 cells. *Diabetes* **56**:204–210 [Abstract/FREE Full Text](#)

13. **Bretscher MS, Munro S** 1993 Cholesterol and the Golgi apparatus. *Science* **261**:1280–1281
[FREE Full Text](#)
14. **Simons K, Ikonen E** 2000 How cells handle cholesterol. *Science* **290**:1721–1726
[Abstract/FREE Full Text](#)
15. **Lodish H, Berk A, Matsudaira P, Kaiser CA, Krieger M, Scott MP, Zipursky SL, Darnell J** 2004 Biomembranes and cell architecture. In: *Molecular cell biology*. 5th ed. New York: Scientific American Press; 147–157
16. **Hosaka M, Suda M, Sakai Y, Izumi T, Watanabe T, Takeuchi T** 2004 Secretogranin III binds to cholesterol in the secretory granule membrane as an adapter for chromogranin A. *J Biol Chem* **279**:3627–3634 [Abstract/FREE Full Text](#)
17. **Arnautova I, Smith AM, Coates LC, Sharpe JC, Dhanvantari S, Snell CR, Birch NP, Loh YP** 2003 The prohormone processing enzyme PC3 is a lipid raft-associated transmembrane protein. *Biochemistry* **42**:10445–10455 [CrossRef](#) [Medline](#)
18. **Blázquez M, Thiele C, Huttner WB, Docherty K, Shennan KIJ** 2000 Involvement of the membrane lipid bilayer in sorting prohormone convertase 2 into the regulated secretory pathway. *Biochem J* **349**:843–852 [Medline](#)
19. **Assadi M, Sharpe JC, Snell C, Loh YP** 2004 The C-terminus of prohormone convertase 2 is sufficient and necessary for Raft association and sorting to the regulated secretory pathway. *Biochemistry* **43**:7798–7807 [CrossRef](#) [Medline](#)
20. **Takeuchi T, Hosaka M** 2008 Sorting mechanism of peptide hormones and biogenesis mechanism of secretory granules by secretogranin III, a cholesterol-binding protein, in endocrine cells. *Curr Diabetes Rev* **4**:31–38 [CrossRef](#) [Medline](#)
21. **Gondré-Lewis MC, Petrache HI, Wassif CA, Harries D, Parsegian A, Porter FD, Loh YP** 2006 Abnormal sterols in cholesterol-deficiency diseases cause secretory granule malformation and decreased membrane curvature. *J Cell Sci* **119**:1876–1885
[Abstract/FREE Full Text](#)
22. **Moriguchi T, Hosaka M, Yosinari A, Ozaki A, Takeuchi T, Shinozuka K** 2009 Cholesterol analogs labeled with novel silylated fluorescent compounds. *Chem Lett* **38**:966–967
[CrossRef](#)
23. **Sawada Y, Zhang B, Okajima F, Izumi T, Takeuchi T** 2001 Parathyroid hormone-related protein increases pancreatic β -cell-specific functions in well-differentiated cells. *Mol Cell Endocrinol* **182**:265–275 [CrossRef](#) [Medline](#)
24. **Ridsdale A, Denis M, Gougeon PY, Ngsee JK, Presley JF, Zha X** 2006 Cholesterol is required for efficient endoplasmic reticulum-to-Golgi transport of secretory membrane proteins. *Mol Biol Cell* **17**:1593–1605 [Abstract/FREE Full Text](#)
25. **Lee J, Lee I, Park C, Kang WK** 2006 Lovastatin-induced RhoA modulation and its effect on senescence in prostate cancer cells. *Biochem Biophys Res Commun* **339**:748–754 [CrossRef](#)
[Medline](#)
26. **Brusselmans K, Timmermans L, Van de Sande T, Van Veldhoven PP, Guan G, Shechter I, Claessens F, Verhoeven G, Swinnen JV** 2007 Squalene synthase, a determinant of Raft-associated cholesterol and modulator of cancer cell proliferation. *J Biol Chem* **282**:18777–18785 [Abstract/FREE Full Text](#)
27. **Proksch GJ, Bonderman DP** 1978 A water-soluble cholesterol derivative for use in augmenting serum control materials. *Clin Chem* **24**:1924–1926 [Abstract/FREE Full Text](#)
28. **Massy ZA, Guijarro C, Oda H, Kasiske BL, Keane WF, O'Donnell MP** 1999 Importance of geranylgeranyl pyrophosphate for mesangial cell DNA synthesis. *Kidney Int Suppl* **71**:80–83
29. **Lerner EC, Qian Y, Hamilton AD, Sebti SM** 1995 Disruption of oncogenic K-Ras4B processing and signaling by a potent geranylgeranyltransferase I inhibitor. *J Biol Chem* **270**:26770–26773 [Abstract/FREE Full Text](#)
30. **Finder JD, Litz JL, Blaskovich MA, McGuire TF, Qian Y, Hamilton AD, Davies P, Sebti SM** 1997 Inhibition of protein geranylgeranylation causes a superinduction of nitric-oxide synthase-2 by interleukin-1 β in vascular smooth muscle cells. *J Biol Chem* **272**:13484–13488
[Abstract/FREE Full Text](#)
31. **Grimmer S, Iversen TG, van Deurs B, Sandvig K** 2000 Endosome to Golgi transport of ricin is regulated by cholesterol. *Mol Biol Cell* **11**:4205–4216 [Abstract/FREE Full Text](#)
32. **Saito E, Wachi H, Sato F, Seyama Y** 2008 7-Ketocholesterol, a major oxysterol, promotes PI-induced vascular calcification in cultured smooth muscle cells. *J Atheroscler Thromb* **15**:130–137 [Medline](#)
33. **Gomi H, Mizutani S, Kasai K, Itoharu S, Izumi T** 2005 Granuphilin molecularly docks insulin granules to the fusion machinery. *J Cell Biol* **171**:99–109 [Abstract/FREE Full Text](#)
34. **Stechly L, Morelle W, Dessein AF, André S, Grard G, Trinel D, Dejonghe MJ, Leteurte E, Drobecq H, Trugnan G, Gabius HJ, Huet G** 2009 Galectin-4-regulated delivery of glycoproteins to the brush border membrane of enterocyte-like cells. *Traffic* **10**:438–450
[CrossRef](#) [Medline](#)
35. **Wang Y, Thiele C, Huttner WB** 2000 Cholesterol is required for the formation of regulated and constitutive secretory vesicles from the trans-Golgi network. *Traffic* **1**:952–962 [CrossRef](#)
[Medline](#)
36. **Han L, Suda M, Tsuzuki K, Wang R, Ohe Y, Hirai H, Watanabe T, Takeuchi T, Hosaka M** 2008 A large form of secretogranin III functions as a sorting receptor for chromogranin A aggregates in C12 cells. *Mol Endocrinol* **22**:1935–1949 [Abstract/FREE Full Text](#)
37. **Thiele C, Hannah MJ, Fahrenholz F, Huttner WB** 2000 Cholesterol binds to synaptophysin and is required for biogenesis of synaptic vesicles. *Nat Cell Biol* **2**:42–49 [CrossRef](#) [Medline](#)
38. **Huang J, Feigenson GW** 1999 A microscopic interaction model of maximum solubility of cholesterol in lipid bilayers. *Biophys J* **76**:2142–2157 [Medline](#)
39. **Wei S, Lee TS, Zhu M, Gu C, Wang Y, Zhu Y, Shyy JY** 2006 Statins activate AMP-activated protein kinase in vitro and in vivo. *Circulation* **114**:2655–2662 [Abstract/FREE Full Text](#)
40. **Viollet B, Mounier R, Leclerc J, Yazigi A, Foretz M, Andreelli F** 2007 Targeting AMP-activated protein kinase as a novel therapeutic approach for the treatment of metabolic disorders. *Diabetes Metab* **33**:395–402 [CrossRef](#) [Medline](#)
41. **Okazaki Y, Eto K, Yamashita T, Okamoto M, Ohsugi M, Noda M, Terauchi Y, Ueki K, Kadawaki T** 2010 Decreased insulin secretion and accumulation of triglyceride in β cells

- overexpressing a dominant-negative form of AMP-activated protein kinase. *Endocr J* **57**:141–152 [CrossRef](#) [Medline](#)
42. **Cole SL, Grudzien A, Manhart IO, Kelly BL, Oakley H, Vassar R** 2005 Statins cause intracellular accumulation of amyloid precursor protein, β -secretase-cleaved fragments, and amyloid β -peptide via an isoprenoid-dependent mechanism. *J Biol Chem* **280**:18755–18770 [Abstract/FREE Full Text](#)
 43. **Chugh A, Ray A, Gupta JB** 2003 Squalene epoxidase as a hypocholesterolemic drug target revisited. *Prog Lipid Res* **42**:37–50 [CrossRef](#) [Medline](#)
 44. **Xia F, Xie L, Mihic A, Gao X, Chen Y, Gaisano HY, Tsushima RG** 2008 Inhibition of cholesterol biosynthesis impairs insulin secretion and voltage-gated calcium channel function in pancreatic β -cells. *Endocrinology* **149**:5136–5145 [Abstract/FREE Full Text](#)
 45. **Tanaka T, Tatsuno I, Uchida D, Moroo I, Morio H, Nakamura S, Noguchi Y, Yasuda T, Kitagawa M, Saito Y, Hirai A** 2000 Geranylgeranyl-pyrophosphate, an isoprenoid of mevalonate cascade, is a critical compound for rat primary cultured cortical neurons to protect the cell death induced by 3-hydroxy-3-methylglutaryl-CoA reductase inhibition. *J Neurosci* **20**:2852–2859 [Abstract/FREE Full Text](#)
 46. **Salaün C, James DJ, Chamberlain LH** 2004 Lipid rafts and the regulation of exocytosis. *Traffic* **5**:255–264 [CrossRef](#) [Medline](#)
 47. **Tooze SA, Martens GJM, Huttner WB** 2001 Secretory granule biogenesis: rafting to the SNARE. *Trends Cell Biol* **11**:16–22 [Medline](#)
 48. **Chamberlain LH, Burgoyne RD, Gould GW** 2001 SNARE proteins are highly enriched in lipid rafts in PC12 cells: Implications for the spatial control of exocytosis. *Proc Natl Acad Sci USA* **98**:5619–5624 [Abstract/FREE Full Text](#)
 49. **Ohara-Imaizumi M, Nishiwaki C, Kikuta T, Kumakura K, Nakamichi Y, Nagamatsu S** 2004 Site of docking and fusion of insulin secretory granules in live MIN6 β -cells analyzed by TAT-conjugated anti-syntaxin 1 antibody and total internal reflection fluorescence microscopy. *J Biol Chem* **279**:8403–8408 [Abstract/FREE Full Text](#)
 50. **Hosaka M, Watanabe T, Sakai Y, Uchiyama Y, Takeuchi T** 2002 Identification of a chromogranin A domain that mediates binding to secretogranin III and targeting to secretory granules in pituitary cells and pancreatic β -cells. *Mol Biol Cell* **13**:3388–3399 [Abstract/FREE Full Text](#)
 51. **Cool DR, Normant E, Shen F, Chen HC, Pannell L, Zhang Y, Loh YP** 1997 Carboxypeptidase E is a regulated secretory pathway sorting receptor: genetic obliteration leads to endocrine disorders in Cpe(fat) mice. *Cell* **88**:73–83 [CrossRef](#) [Medline](#)
 52. **Hosaka M, Watanabe T, Sakai Y, Kato T, Takeuchi T** 2005 Interaction between secretogranin III and carboxypeptidase E facilitates prohormone sorting within secretory granules. *J Cell Sci* **118**:4785–4795 [Abstract/FREE Full Text](#)
 53. **Farsad K, De Camilli P** 2003 Mechanisms of membrane deformation. *Curr Opin Cell Biol* **15**:372–381 [CrossRef](#) [Medline](#)
 54. **Horton JD, Goldstein JL, Brown MS** 2002 SREBPs: activators of the complete program of cholesterol and fatty acid synthesis in the liver. *J Clin Invest* **109**:1125–1131 [CrossRef](#) [Medline](#)

Articles citing this article

FoxO1 as a double-edged sword in the pancreas: analysis of pancreas- and β -cell-specific FoxO1 knockout mice

Am. J. Physiol. Endocrinol. Metab. 2012 302: E603-E613

[Abstract](#) [Full Text](#) [Full Text \(PDF\)](#)